Tissue and Cell 101 (2026) 103403

Contents lists available at ScienceDirect

Tissue and Cell

journal homepage: www.elsevier.com/locate/tice

Sperm morphology and ultrastructure in four species of ground beetles (Insects-Carabidae)☆

Mariangela Gentile [a], David Mercati [a], Pietro Brandmayr [b], Andrea Di Giulio [c], Pietro Lupetti [a], Romano Dallai [a,*]

[a] Department of Life Sciences, University of Siena, Siena, Italy
[b] Department of Biology, Ecology and Earth Sciences, Di.B.E.S.T., University of Calabria, Cosenza, Italy
[c] Department of Science, Roma Tre University, Rome, Italy

ARTICLE INFO

Keywords:
Insect sperm ultrastructure
Carabidae
Electron microscopy

ABSTRACT

Ground beetles (Carabidae) exhibit diverse sperm morphologies, ranging from free cells to conjugated bundles embedded in spermatostyles. Detailed ultrastructural analyses of four species - *Paussus favieri* (Paussinae), *Tachys scutellaris* and *Pogonus littoralis* (Trechinae), and *Laemostenus acutangulus* (Harpalinae) - were conducted using transmission electron and fluorescence microscopy. Free sperm were observed in *P. favieri*, *T. scutellaris*, and *P. littoralis*, with notable features including a monostratified acrosome and polysaccharide-rich granular material in *P. favieri*, and unique accessory bodies in *T. scutellaris*. *L. acutangulus* displayed sperm conjugated within crystallized spermatostyles, suggesting the presence of enzymatic proteins. These findings reveal structural diversity linked to phylogenetic positions, suggesting that free sperm predominate in basal lineages, while conjugated sperm with spermatostyles are characteristic of higher Carabidae. The study enhances understanding of sperm evolution and reproductive adaptations in ground beetles, providing a foundation for future comparative and systematic investigations. As a final consideration, it was hypothesized that sperm conjugation could be the ancestral condition of insect reproduction.

1. Introduction

Carabidae exhibit remarkable diversity in the arrangement of their sperm following spermiogenesis, particularly as sperm traverse the deferent duct. Sperm may exist as free cells or aggregate into complex bundles known as spermatozeugmata, in which the sperm heads are embedded within dense structures secreted by the deferent duct epithelium termed spermatostyles (Higginson and Pitnick, 2011). These structures, vary in size, shape, and the manner in which they attach to and protect sperm. Typically, spermatostyles are rod-shaped, though in some groups they may take on a cap-like form (Carcupino et al., 2002; Takami, 2002; Takami and Sota, 2007; Sasakawa, 2007; Hodgson et al., 2013; Schubert et al., 2017; Dallai et al., 2019, 2020; Gómez and Maddison, 2020). Recent work (Lupetti et al., 2024) suggests that both cap- and rod-shaped spermatostyles share a common origin, despite their differing final morphologies. Within Carabidae, some groups, such as Apotomini (Gómez et al., 2023), Cicindelini, Notiophilini, and Nebriini (Dallai et al., 2020), possess only free sperm, while many other groups contain both singleton and conjugated sperm. This dual presence has been described in subfamilies including Trechinae, Harpalinae, Paussinae, Broscinae (Gómez and Maddison, 2020), Rhysodinae (Giglio et al., 2024), and others (Gómez and Maddison, 2020). Based on these findings, it has been hypothesized that sperm conjugation, in addition to facilitating the transport of large numbers of sperm to the female during mating (Breland and Simmons, 1970; Afzelius and Dallai, 1987) and enhancing competitive fertilization success (Moore and Moore, 2002), may confer other advantages. However, none of these proposed benefits have been conclusively supported (Higginson and Pitnick, 2011). Sperm conjugation is also considered an ancestral form of sperm organization in diving and whirligig beetles, and this aggregation is observed in other insect groups as well (Higginson and Pitnick, 2011; Higginson et al., 2012). Evidence from Yager (1981, 1989) indicates that Remipedia, an

☆ Given his role as Editor, Pietro Lupetti had no involvement in the peer-review of this article and has no access to information regarding its peer-review. Full responsibility for the editorial process for this article was delegated to another journal editor.

* Corresponding author.
E-mail addresses: mariangela.gentile@unisi.it (M. Gentile), david.mercati@unisi.it (D. Mercati), brandmayr@unical.it (P. Brandmayr), andrea.digiulio@uniroma3.it (A. Di Giulio), pietro.lupetti@unisi.it (P. Lupetti), romano.dallai@unisi.it (R. Dallai).

https://doi.org/10.1016/j.tice.2026.103403
Received 23 December 2025; Received in revised form 17 February 2026; Accepted 18 February 2026
Available online 19 February 2026

ancient group of Crustacea considered ancestral to Hexapoda, produces spermatophores containing 3–6 sperm each, supporting the hypothesis of an ancestral origin for sperm conjugation (von Reumont et al., 2009; Regier et al., 2010; Giribet and Edgecombe, 2012; Tihelka et al., 2021).

In this study, we provide detailed ultrastructural descriptions of sperm from additional members of the Carabidae, including both singleton and conjugated forms. These new data contribute to a better understanding of sperm diversity within the family and may help clarify relationships among the various carabid groups examined to date.

2. Materials and methods

2.1. Species were studied for the present work

Males and females of *Paussus favieri* Fairmaire, 1851, were collected in 2010 from nests of *Pheidole pallidula* found under stones in a Mediterranean garrigue in the High Atlas Mountains by Andrea Di Giulio.

Males and females of *Tachys scutellaris* Stephens, 1828, were collected in 2024 in the saltmarshes with *Salicornia* near Monfalcone (northern Italy) by Pietro Brandmayr.

Males of *Laemostenus (Actenipus) acutangulus* (Schaufuss, 1862) were collected in 2025 near Cosenza, Calabria, Italy by Pietro Brandmayr.

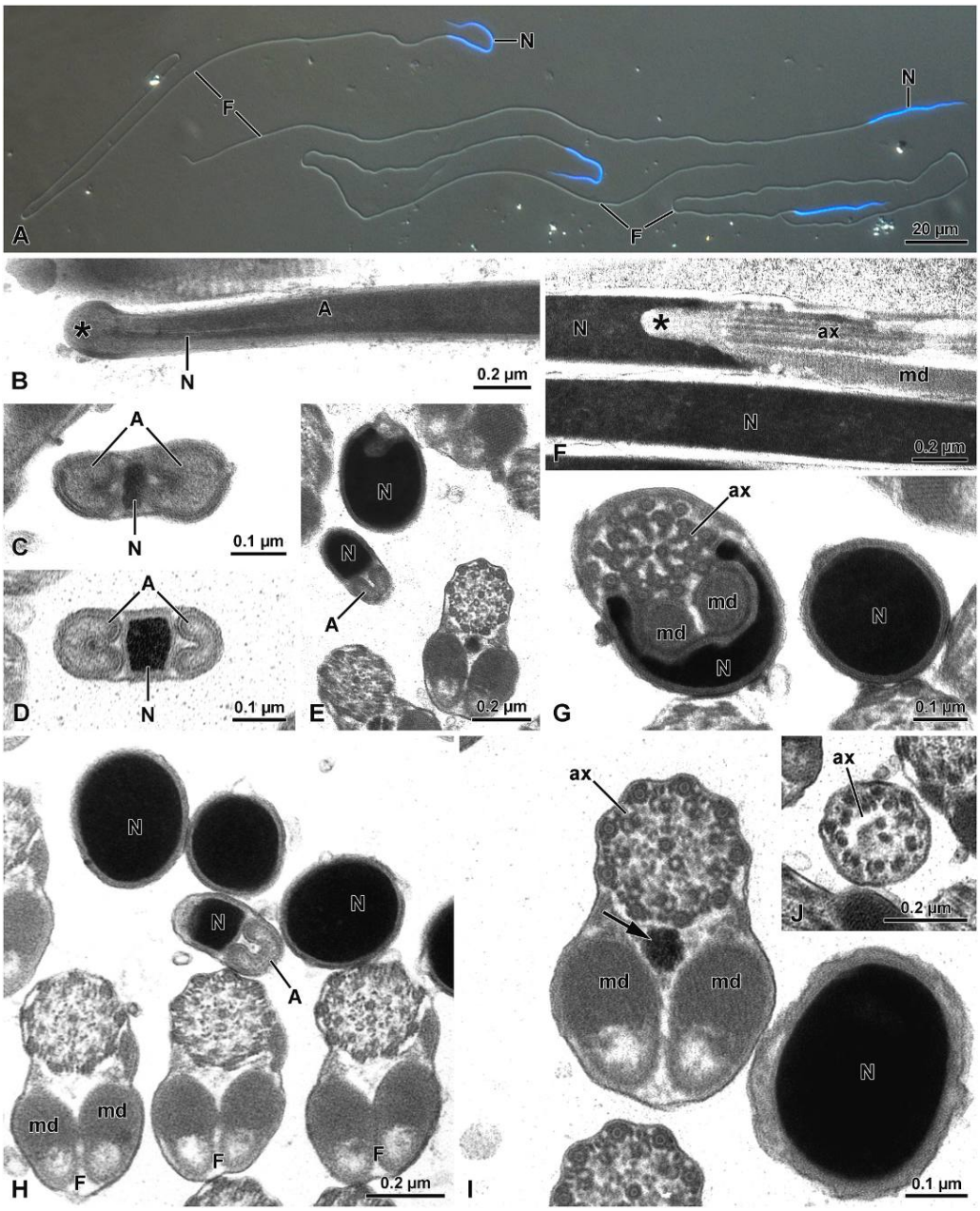

Fig. 1. *Paussus favieri.* **A)** Hoechst staining of sperm. Note the apical nucleus and the long flagella. **B)** Longitudinal section showing the acrosome running lateral to the nucleus. Note the apical fusion of the acrosomal vesicle (asterisk). **C, D)** Cross section of the apical nuclear region showing the acrosome vesicle on both sides of the nucleus. **E)** Cross section through two levels of the nucleus. **F)** Longitudinal section through the posterior nuclear region. Note the nuclear cavity hosting the basal body and the beginning of the axoneme embedded in the centriole adjunct material (asterisk). On the opposite side the mitochondrial derivative is visible. **G)** Cross section of the posterior nuclear region and the beginning of the flagellar axoneme. **H)** Cross section showing nuclei at different levels and three flagella without the axial electron-dense material. **I)** Cross section through a flagellar axoneme with the axial electron-dense granular material (asterisk). **J)** Cross section of the flagellar end with the disorganized axoneme (ax). A, acrosome; ax; axoneme; F, flagella; md, mitochondrial derivatives; N, nucleus.

Males of *Pogonus littoralis* (Duftschmid, 1812) were collected in Valle Canale, Abruzzo (central Italy), in June of 1996 by Giuseppe Osella.

2.2. Fluorescence microscopy

Deferent duct of *T. scutellaris* and free sperm of *P. favieri* taken from the last part of deferent ducts of adult males, were placed over a glass in a small drop of 0.1 M phosphate buffer (pH 7.2) to which 3 % of sucrose was previously added (PB), squashed with a coverslip and observed and photographed with a Leica DMRB interference contrast and epifluorescent microscope equipped with an AxioCam HR camera (Carl Zeiss). DNA was stained for fluorescence observations by incubating the material for 3–4 min in Hoechst 33258 1 μg/ml (Sigma). The material was then mounted in a drop of 90 % glycerol.

2.3. Transmission electron microscopy

Males of all the species here examined were dissected in 0.1 M PB. After dissection, the whole reproductive system was removed and the testes, deferent ducts and seminal vesicles were isolated. The material was fixed overnight in 2.5 % glutaraldehyde in PB at 4 °C. After rinsing in PB, the material was post-fixed for two hours in 1 % of osmium tetroxide in PB at 4 °C. After rinsing in PB, the material was dehydrated in an ascending alcohol series, then transferred into propylene oxide and finally embedded in Epon-Araldite resin mixture. Ultrathin sections (50–60 nm), obtained with a Reichert Ultracut ultramicrotome, were stained routinely with uranyl acetate and lead citrate. Polysaccharides in *P. favieri* sperm were detected by the periodic acid-thiosemicarbazide-silver proteinate method (Thiéry, 1967). All observations were performed with a Philips CM10 transmission electron microscope operating at an accelerating voltage of 80 kV.

3. Results

3.1. Paussus favieri Fairmaire, 1851 (Paussinae – Paussini)

The sperm ultrastructure of the ground beetle *Paussus favieri* represents the first record of free spermatozoa within the tribe Paussini; however, this tribe also includes species with sperm aggregates (Gómez and Maddison, 2020). The sperm was relatively long, measuring approximately 165 μm, and consisted of an apical acrosome of about 0.94 μm, a nucleus 33 μm in length, and a long flagellum (Fig. 1A).

The acrosome was a thin, cylindrical structure, about 45 nm thick in cross section, bent to form a saddle-shaped configuration positioned laterally to the apical region of the nucleus (Fig. 1B–E, H). Depending on the level of sectioning, this configuration appeared on one (proximal) (Fig. 1E, H) or on both (distal) sides of the anterior nuclear region (Fig. 1B–D). At the distal end of the nucleus, a rounded cap, approximately 0.34 μm wide, was visible; this structure resulted from the fusion of the two acrosomal saddles located on opposite sides of the nucleus (Fig. 1B–D). No perforatorium was apparent, as the acrosome was monostratified.

The nucleus was an elongated, cylindrical structure measuring 0.34 μm in cross section at its basal region (Fig. 1F) and narrowing to about 60 nm at the tip, where it was flanked by the two lateral acrosomal saddles (Fig. 1C, D). The chromatin within the nucleus was compact and highly electron-dense (Fig. 1C–I). In the proximal region, the nucleus exhibited a deep cavity that housed the basal body and flagellum on one side and the two mitochondrial derivatives on the other (Fig. 1F, G). This entire region contained electron-dense material associated with the centriole adjunct, which intermingled with the surrounding organelles (Fig. 1F, G).

In cross section, the flagellum displayed the conventional 9 + 9 + 2 microtubular axonemal pattern, with electron-dense accessory tubules (Fig. 1G–I; 2 A). Beneath the axoneme lay two equal, elliptical mitochondrial derivatives, whose surfaces facing the axoneme exhibited electron-dense crystallization (Fig. 1H, I; 2 A). Two small cisternae were visible at their apical regions. Two accessory bodies were present: the one on the right side was 0.11 μm long and elliptical in shape, whereas the one on the opposite side consisted of a less conspicuous amount of material (Fig. 1H; 2 A). The accessory bodies appeared to be restricted to the anterior region of the flagellum (Fig. 1I).

The mitochondrial derivatives were helically arranged around the axoneme. An unusual ultrastructural feature of the flagellum was the presence of electron-dense granular material along its axial region, located in the space between the axoneme and the anterior parts of the mitochondrial derivatives (Fig. 1I; 2A–D). This material consisted of aggregates of three to six small electron-dense granules (Fig. 1I; 2A–D). Notably, these granules were distributed along the flagellum with a periodicity of 35–70 nm, such that they were visible only in certain cross sections and absent in others (compare Fig. 1H and Fig. 2A). The Thiéry method for the detection of polysaccharides gave a positive reaction, thus suggesting that this material could represent a source of energy for flagellar motility (Fig. 2C, D).

Towards the posterior region of the flagellum, the two mitochondrial derivatives gradually decreased in size, eventually leaving only one derivative before disappearing entirely. The terminal portion of the tail displayed only a disorganized flagellar axoneme (Fig. 1J).

Within the female spermatheca, the ultrastructural organization of the sperm described above was not altered.

3.2. Tachys scutellaris Stephens, 1828 (Trechinae – Bembidiini)

The sperm of *Tachys scutellaris* was a relatively long cell, although its full length could not be identified due to the narrow and extremely long deferent ducts (Fig. 3A, B). The acrosome was short, and the cylindrical nucleus measured approximately 35 μm in length and 0.25 μm in width (Fig. 3C). The basal nuclear region was adapted to accommodate the two equal mitochondrial derivatives on one side and the basal body and flagellar axoneme on the opposite side. The flagellar axoneme exhibited the conventional 9 + 9 + 2 pattern with electron-dense accessory tubules (Fig. 3E–G). The two mitochondrial derivatives had an unusual shape in cross section, extending their dorsal region to embrace the axoneme (Fig. 3E–G). Their matrix was also distinctive, showing a crystallized central region, about 0.15 μm in diameter, differing from the peripheral region, and containing an electron-dense axis (Fig. 3E–G).

The two accessory bodies represented the most peculiar structures. Generally, these consisted of relatively small electron-dense structures located between the axoneme and the mitochondrial derivatives. In *T. scutellaris*, by contrast, they appeared in cross section as two electron-dense laminae, only 0.10 μm thick, adhering to the inner face of the mitochondrial derivatives and following the outline of the outer microtubular structure of the axoneme (Fig. 3E–G). Moreover, their upper extremities slightly expanded (0.20 μm wide) to form a thicker structure (Fig. 3F). In longitudinal section, the mitochondrial derivatives were arranged helically around the axoneme, with a periodicity of about 3.12 μm. In the posterior tail region, they gradually decreased in size and eventually disappeared. The tail end contained only the axoneme (Fig. 3G).

3.3. Pogonus littoralis (Duftschmid, 1812) (Trechinae – Pogonini)

The nearly mature sperm of *Pogonus littoralis* were long, free cells lacking an acrosome. Anteriorly, the sperm exhibited an empty structure that, slightly posteriorly, became very large (about 2.5 μm wide) and showed, in its inner region, a thick prismatic body (0.62 μm wide) (Fig. 4A–F). This structure further modified its shape to host and protect the basal body and axoneme dorsally and the nucleus in a ventral position. More posteriorly, the prismatic structure became smaller and opened to give rise to a thick band surrounding the microtubular elements of the axoneme, which progressively became complete (Fig. 4G–M).

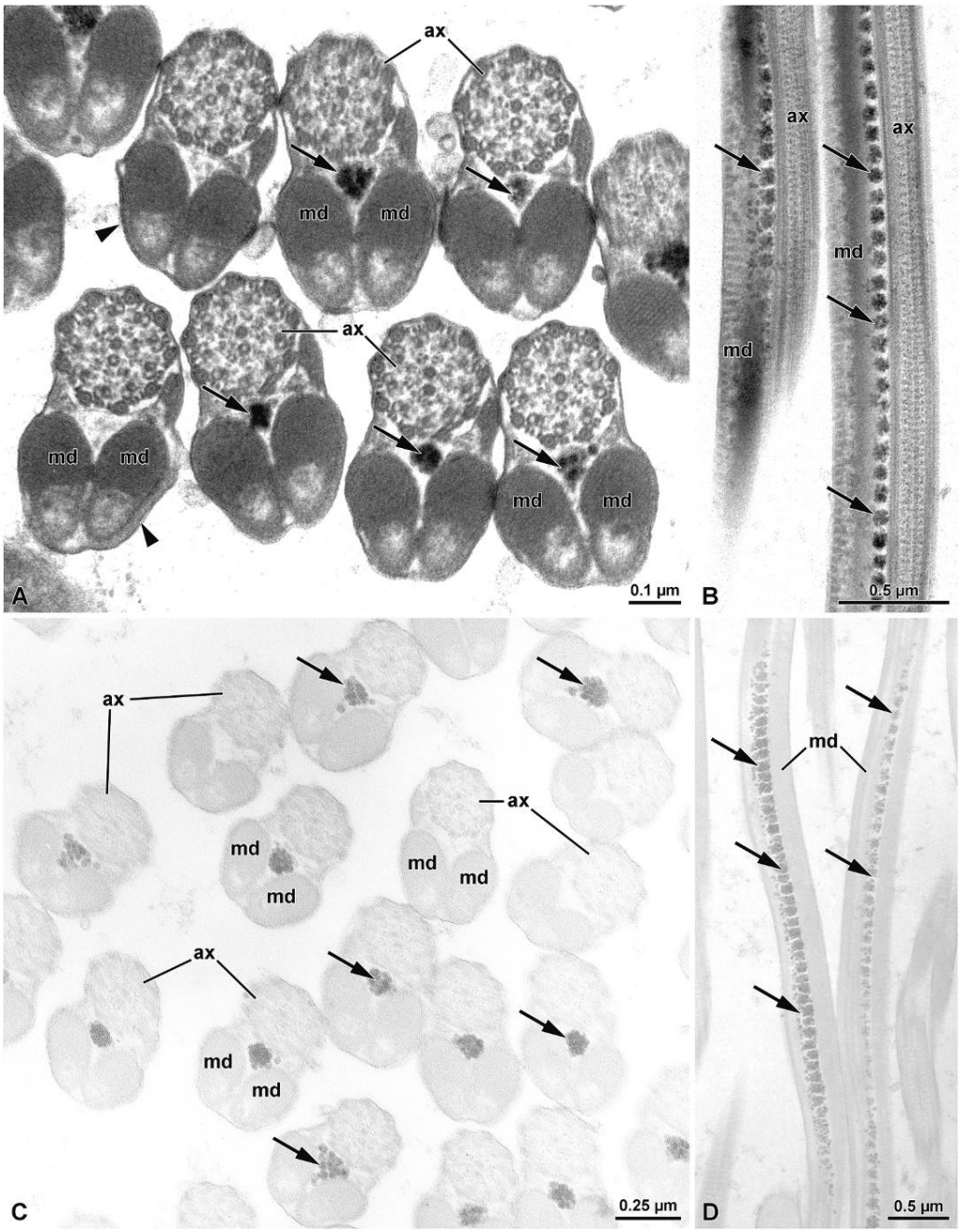

Fig. 2. *Paussus favieri*. **A)** Cross section of a flagellar bundle with some flagella with the axial electron-dense granular material (arrows) and others without this material (arrowheads). **B)** Longitudinal section of a flagellum with mitochondrial derivatives and the axial region (arrows) showing the regular distribution of the electron-dense granular material. **C, D)** Cross and longitudinal sections of the flagellum showing the positivity to Thiéry methods for polysaccharides of the electron-dense material along the axial region of the flagellar axoneme (arrows). ax; axoneme; md, mitochondrial derivatives; N, nucleus.

At the same time, beneath the axoneme, a small (about 62 nm) elliptical nucleus became evident in cross section (Fig. 4H–M). On both sides of the nucleus, two small electron-dense bodies, possibly mitochondrial derivatives, were present (Fig. 4O). In cross section through the middle region of an almost mature sperm, three structures were visible in an orderly parallel sequence: dorsally the axoneme, in the middle region the two equal mitochondrial derivatives, and ventrally the nucleus with chromatin still uncondensed (Fig. 5A–D). These components were surrounded by microtubules (Fig. 5A–D). On the right side of the axoneme, a small spherical accessory body (62 nm wide) was visible (Fig. 5B–D).

The two mitochondrial derivatives had an elliptical shape in cross section and, depending on the level of sectioning, their size varied from 0.35 µm × 0.18 µm to 0.31 µm × 0.17 µm. Two small electron-dense bodies were visible beneath them (Fig. 5B, D). The nucleus also had an elliptical shape (0.5 µm × 0.4 µm), and its content exhibited an electron-dense complex of chromatin filaments (Fig. 5A–D). In more posterior regions, the mitochondrial derivatives reduced in size, becoming globular in cross section (0.16 µm in diameter), and the nucleus reached approximately the same diameter (Fig. 5D). In the final stage of spermatid maturation, the sperm showed, in cross section, a classic axoneme with a 9 + 9 + 2 microtubular complex, two elongated mitochondrial derivatives with a matrix of uniform electron-dense material, and an elliptical nucleus with two electron-dense lateral dots of 23 nm each, apparently corresponding to contact points with the ventral regions of the mitochondrial derivatives (Fig. 5E). On the right side of

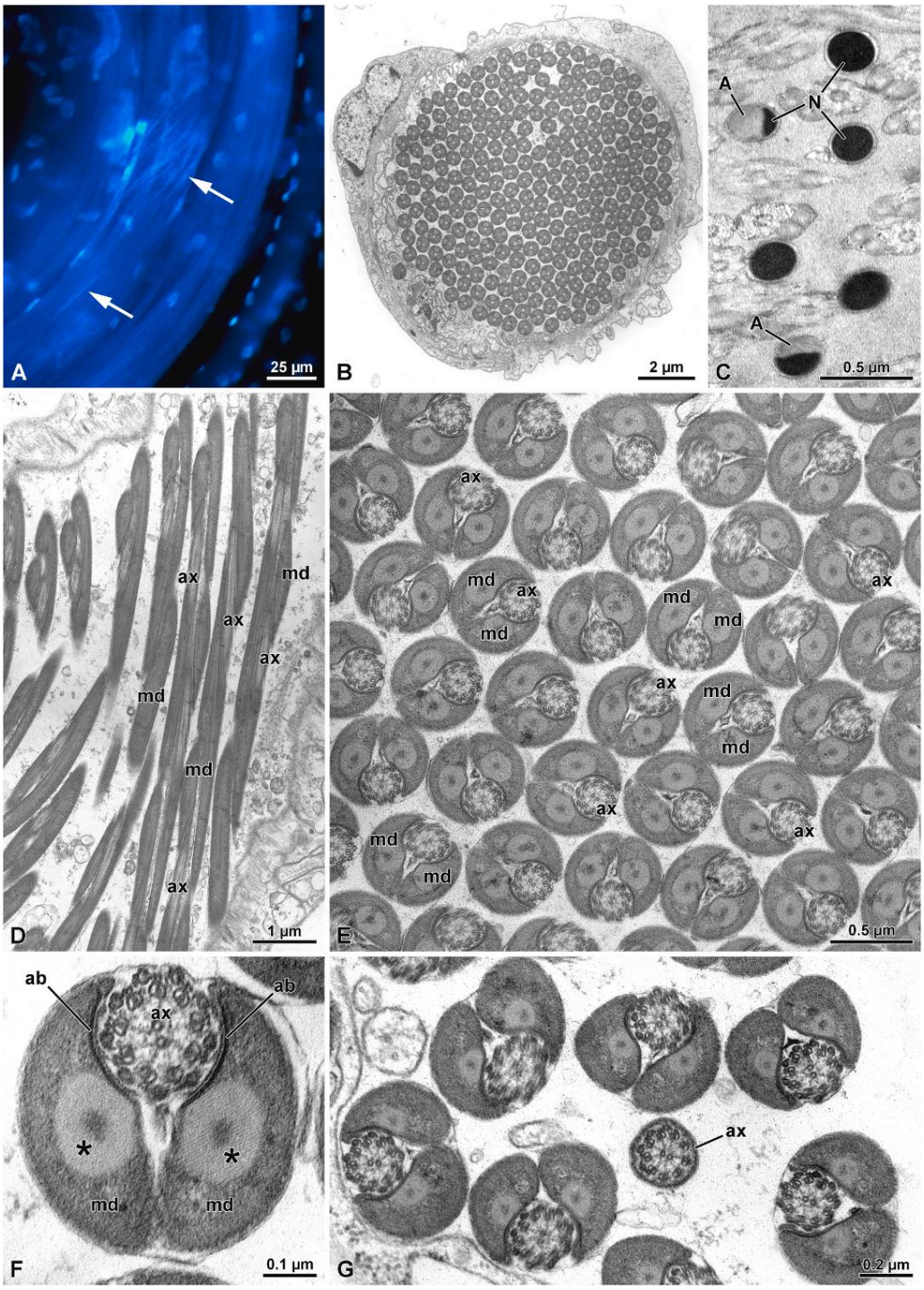

Fig. 3. *Tachys scutellaris*. **A)** Hoechst staining of the extremely long deferent duct of specimens. Note the nuclei (arrows) within the duct lumen. **B)** Cross section of a deferent duct filled with sperm flagella. **C)** Cross section of acrosome and nucleus in the spermathecal lumen. **D)** Longitudinal sections of flagella in the deferent duct. Note the helicoidal array of mitochondrial derivatives around axoneme. **E)** Cross section through flagella within a deferent duct. Note the equal mitochondrial derivatives embracing the axoneme. **F)** Higher magnification of a flagellum cross section. Note the laminar structure of the accessory bodies adhering to the inner face of the mitochondrial derivatives which present their central part crystallized (asterisks). **G)** Cross section of a flagellum end with only the axoneme. A, acrosome; ab, accessory bodies; ax; axoneme; md, mitochondrial derivatives; N, nucleus.

the axoneme, a small elliptical accessory body was visible (Fig. 5E). The tail end showed only the axoneme and, beneath it, a small flattened nucleus.

3.4. Laemostenus (Actenipus) acutangulus (Schaufuss, 1862) (Harpalinae – Sphodrini)

This species, like other Sphodrini, possessed conjugated sperm organized into elongated spermatostyles. These structures had a variable length, reaching up to 300–400 µm. Sperm cells, about 150 µm long, were adherent by their head regions to the peripheral, uniformly

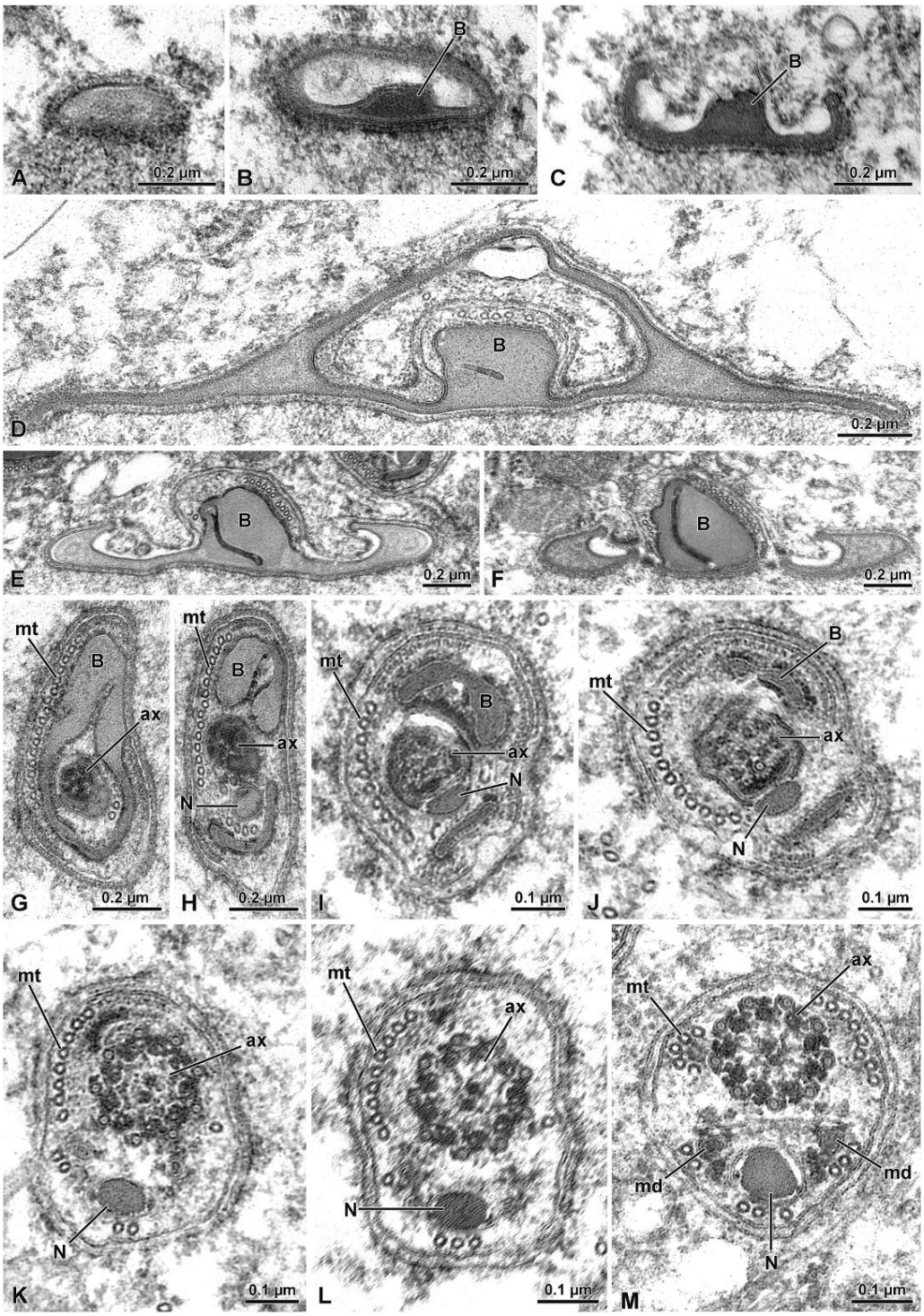

Fig. 4. *Pogonus littoralis*. **A-F)** Serial cross sections through the anterior sperm region. Note the shape and its modifications of the prismatic body where the axoneme and nucleus take origin. **G-L)** Serial cross sections showing the progressive development of the axoneme and, beneath it, of the nucleus. The complex structure is surrounded by microtubules. **M)** Cross section of a spermatid flagellum with the complete axoneme, the nucleus and the two electron-dense bodies, possibly of mitochondrial derivatives. ax; axoneme; B, prismatic body; md, mitochondrial derivatives; mt, microtubules; N, nucleus.

electron-dense material of the spermatostyle (Fig. 6A–D). By contrast, the inner region of this structure consisted of material with a more organized architecture, apparently compact and crystallized in appearance (Fig. 6D, E). At higher magnification, this material showed parallel short electron-dense lines forming ribbons of variable length (Fig. 6E).

The apical extremity of the spermatostyle had a different appearance, due to the scarcity of electron-dense material and the presence of large empty spaces (Fig. 6H–I). In this region, sperm were absent or very rare and, when present, incorrectly oriented (Fig. 6H–I). As in other members of the tribe, electron-dense laminae, 0.66 nm thick, detached from the periphery of the spermatostyle and surrounded areas hosting single or few sperm (Fig. 6B–D).

The sperm heads, embedded within the peripheral material of the spermatostyle, had a flattened apical acrosome consisting of a

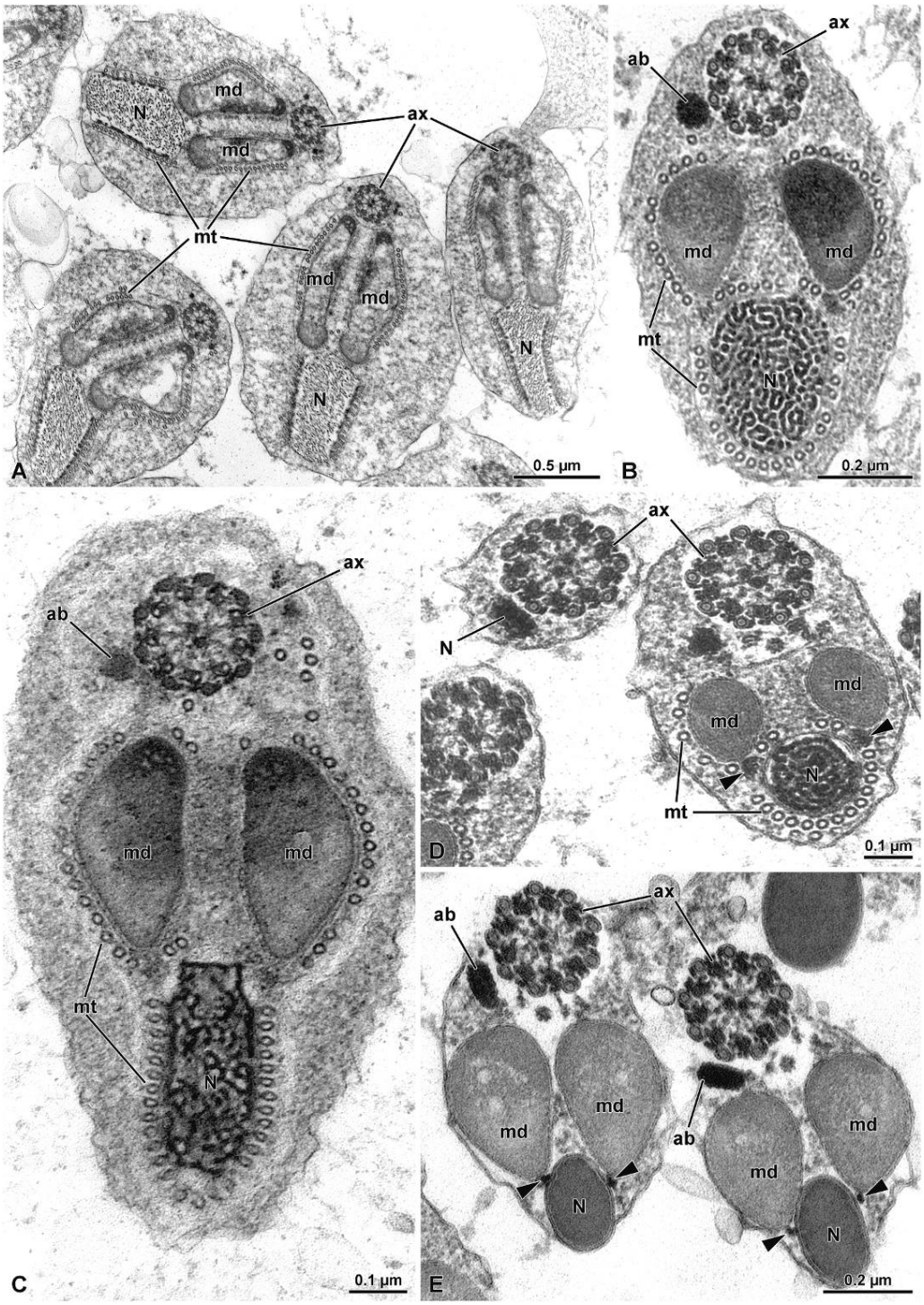

Fig. 5. *Pogonus littoralis*. **A-D)** Serial cross sections through the spermatids maturation. Dorsal axoneme, mitochondrial derivatives and ventral nucleus are in parallel order along the flagellar length. The two last structures are surrounded by microtubules. on the right side of the axoneme a cylindrical accessory body is visible. Two dense bodies are lateral to the nucleus (arrowheads). **E)** Cross section of sperm with axoneme, accessory body, mitochondrial derivatives and the ventral nucleus. Two small dense bodies (arrowheads) are lateral to the nucleus close to the ventral side of the mitochondrial derivatives. ab, accessory bodies; ax; axoneme; md, mitochondrial derivatives; mt, microtubules; N, nucleus.

monolayered structure, 0.52 µm long and 0.10 µm thick. A cross section through the anterior extremity of the acrosome showed a flat vesicle surrounded by the plasma membrane (Fig. 6D, E). Slightly posterior to this region, the apical nuclear tip was visible. The nucleus then assumed an arrow-shaped profile, 0.24 µm thick, and more posteriorly a rectangular shape, 0.15 µm × 90 nm, with compact electron-dense chromatin (Fig. 6D, E). In more posterior regions, distant from the spermatostyle, the cylindrical nucleus, circular in cross section, measured 0.25 µm in diameter and occupied a ventral position, parallel to the flagellar axoneme and the two mitochondrial derivatives for most of the sperm length (Fig. 6F). The flagellar axoneme occupied a dorsal position (Fig. 6F). It originated at the posterior acrosomal region and exhibited the conventional 9 + 9 + 2 microtubular pattern (Fig. 6F).

The two equal mitochondrial derivatives, measuring 0.22 µm

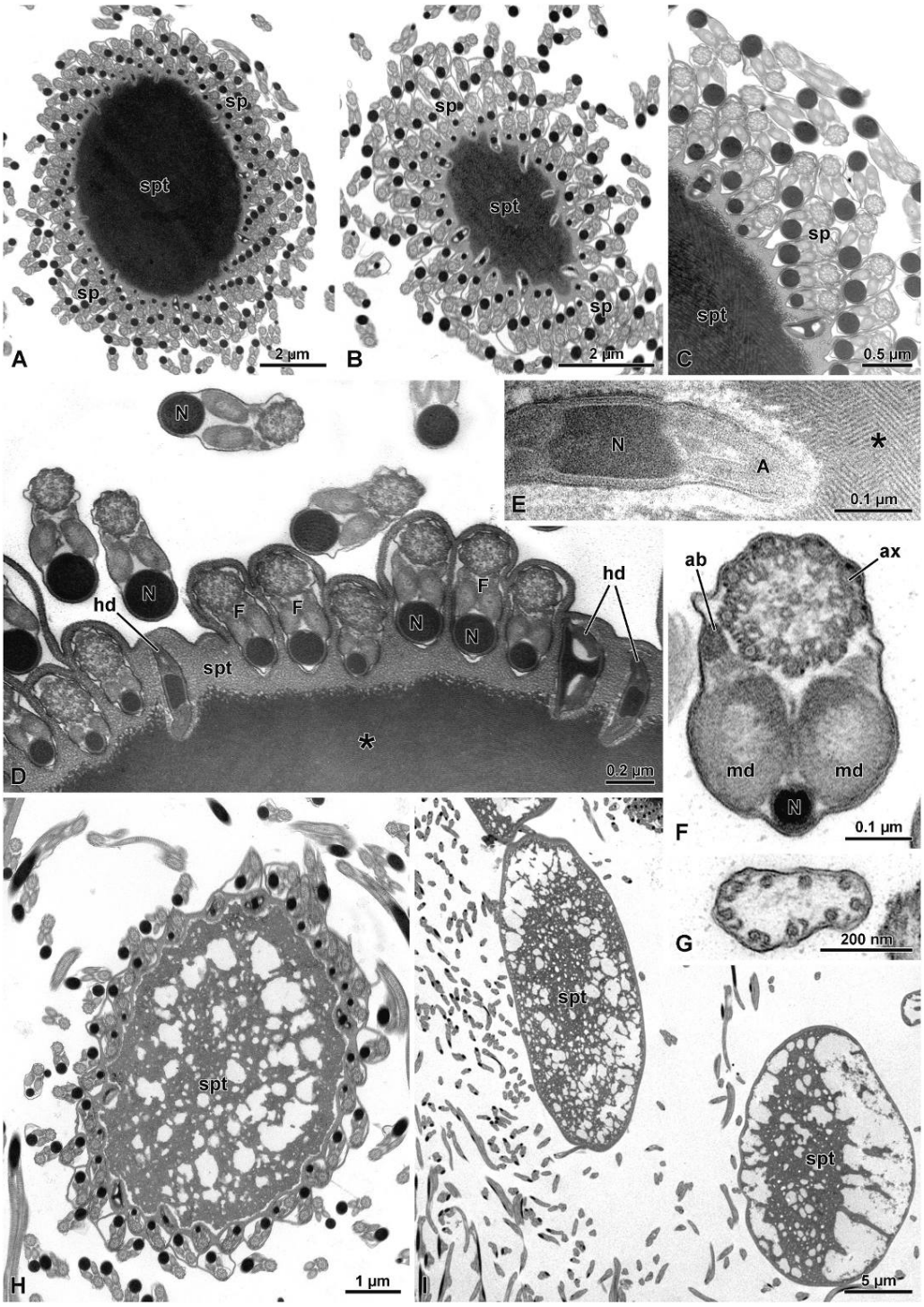

Fig. 6. *Laemostenus (Actenipus) acutangulus*. **A)** Cross section through a spermatostyle on which many sperm are attached. **B)** Cross section through a spermatostyle (spt) posterior end with many sperm attached. **C)** Detail of the complex of sperm attached to the central region of the spermatostyle. **D)** The periphery of the spermatostyle has a uniform structure compared to the inner electron-dense region (asterisk). In the former are attached the sperm with their head region and their ventral region of the sperm flagella. **E)** Higher magnification of a sperm head region with acrosome and nucleus to show the complex structure of the inner region of the spermatostyle consisting of crystallized material (asterisk). **F)** Cross section of a sperm flagellum with the axoneme, accessory body, two equal mitochondrial derivatives and the ventral nucleus. **G)** Cross section through the tail end with some residual axonemal microtubules beneath the plasma membrane. **H, I)** Cross sections of the apical extremity of three spermatostyles with a scarce presence of inner material and the presence of many empty spaces. On these regions the sperm are few and with a wrong orientation. A, acrosome; ab, accessory bodies; ax; axoneme; F, flagella; hd, sperm head region; md, mitochondrial derivatives; N, nucleus; sp, sperm; spt, spermatostyle.

× 0.10 μm, accompanied the axoneme up to the posterior tail end, where they disappeared, leaving only the axoneme visible. In this region, the axonemal microtubules also appeared disorganized, with only a few microtubules remaining visible (Fig. 6G). Two accessory bodies were located in the anterior flagellar region between the axoneme and the mitochondrial derivatives. The one on the right side was larger than the opposite one and had a triangular shape in cross section (0.58 μm × 0.35 μm) (Fig. 6F).

4. Discussion

4.1. Comparative analysis of the sperm structure

The four species examined in this study represent different groups of ground beetles: two are members of Trechinae (*Pogonus littoralis* and *Tachys scutellaris*), one belongs to Paussinae (*Paussus favieri*), and one is a member of Sphodrini, part of the 'higher Carabidae' subfamily Harpalinae (*Laemostenus (Actenipus) acutangulus*). This study adds to our understanding of sperm ultrastructure within the diverse Carabidae (Werner, 1965; Carcupino et al., 2002; Takami and Sota, 2007; Sasakawa, 2009; Hodgson et al., 2013; Schubert et al., 2017; Dallai et al., 2019, 2020; Gómez and Maddison, 2020; Gómez et al., 2024). Our findings reveal two distinct types of sperm organization among the species examined: *P. favieri*, *P. littoralis*, and *T. scutellaris* possess free sperm, while the Harpalinae species *L. acutangulus* has sperm organized in bundles, with their heads embedded in extracellular material known as the spermatostyle. Spermatostyles are unique structures that can take the form of elongated rods or large apical caps, serving to protect the heads of long sperm (Hayashi, 1998; Hayashi and Kamimura, 2002; Higginson and Pitnick, 2011). Recent research has shown that these cap- and rod-shaped structures are homologous, sharing a common origin, with their differentiation occurring only at the final stage of their formation (Lupetti et al., 2024). Two species among those with free sperm belong to the same subfamily Trechinae, but show sperm components with a quite different organization. *T. scutellaris* has a simple and typical sequence of the sperm structures with the acrosome in apical position followed by the nucleus and then the flagellar axoneme. This species, however, has accessory bodies quite similar to those described in *Apotomus rufus* (Gómez et al., 2023) which belongs to the different subfamily Apotominae. On the contrary, *P. littoralis*, as other Trechinae, such as *Duvalius andreinii* and *Anillus florentinus* (Dallai et al., 2020) have axoneme and nucleus running in parallel along the sperm posterior region. In this comparative analysis it was also remarkable the uncommon absence of an acrosome either in *P. littoralis* and *Anillus florentinus*. In the third Trechinae species, *P. favieri*, we observed a distinctive granular aggregation in the axial flagellar region that is positive for polysaccharide staining - a feature not previously described in other Carabidae. This species also possesses an unusual monolayered acrosome, formed by a bent vesicle arranged on both sides of the nucleus.

The parallel arrangement of the axoneme and nucleus along the posterior sperm region, seen in *P. littoralis*, is not unique to that species but is also found in Cicindelinae (Werner, 1965; Dallai et al., 2020), which have free sperm, as well as in several other Carabidae species with conjugated sperm and spermatostyles. All the species of Pterostichinae and Harpalinae have this type of organization (Carcupino et al., 2002; Sasakawa, 2009; Hodgson et al., 2013; Schubert et al., 2017; Dallai et al., 2019, 2020; Gómez and Maddison, 2020). The sperm structure of *L. acutangulus* (tribe Sphodrini) closely resembles that of other Sphodrini species, such as *Calathus latus* and *C. montivagus* (Dallai et al., 2020), which are related to Pterostichini. The spermatostyle in this species, when examined at higher magnification, reveals an inner region with a previously undescribed structure, consisting of numerous short, electron-dense ribbons that suggest the presence of crystallized proteins. The chemical composition of the spermatostyle was recently detected by Gómez et al. (2024) in some whirligig beetles and it is possible that a similar protein composition is also present in the adephagan Carabidae. Moreover, the mentioned work describes also the presence in the spermatostyles of some aminopeptidases and these enzymes could be important, after mating, for the sperm dissociation from the spermatostyle (Breland and Simmons, 1970; Gustafson and Miller, 2017), confirming the general hypothesis that spermatostyles are involved in post-mating functions (Pitnick et al., 2020). The spermatostyle of *L. acutangulus*, as it occurs in other species with a similar structure, prolongs anteriorly in an appendage of reduced diameter characterized by the absence of a uniform structure. Large cavities are present in the inner region. Interesting, at this level, only few sperm or any are visible and the few of them do not have a proper position. Evidently, the absence of the inner compact material of the spermatostyle represents a serious obstacle for the correct insertion of the sperm heads.

4.2. Comparative Considerations on Sperm Aggregation and Free Spermatozoa

The coexistence of both free sperm and conjugated sperm with spermatostyles within related groups raises the intriguing question of which organizational form is ancestral. This issue remains unresolved. Several studies have proposed potential advantages for conjugated sperm organization (see Higginson and Pitnick, 2011), such as facilitating the transfer of large numbers of sperm to the female during mating (Breland and Simmons, 1970; Dallai and Afzelius, 1985; Afzelius and Dallai, 1987). Sperm conjugation would also enable more rapid movement of sperm bundles (Woolley et al., 2009), although the latter observation is based on *in vitro* studies of bull, mouse, rat, fishfly, and firebrat sperm (Bawa and Kanwar, 1975; Hayashi, 1998; Moore and Moore, 2002; Immler et al., 2007; Fisher and Hoekstra, 2010). However, none of these hypotheses has been conclusively supported (Higginson and Pitnick, 2011). The conjugated sperm, after mating, are stored in the female spermatheca waiting egg fertilization. For this event, the sperm must be detached from the spermatostyle to become free to move towards the site of fertilization; the presence of proteolytic enzymes in the spermatostyle (Gómez et al., 2024) could support such a function. Some fragments of spermatostyle material were found in the spermatheca around the sperm bundles of the hydroporine *Stictonectes* (Dallai et al. 2023). The answer to the question on which was the ancestral model between free sperm and those conjugated and with a spermatostyle is not clear and it can be only hypothesized considering the mode of reproduction of old groups related to insects. Among these, Remipedia, the group that morphological and molecular data considered the closest living relatives of insects (von Reumont et al., 2009; Regier et al., 2010; Giribet and Edgecombe, 2012; Tihelka et al., 2021), could be a good example supporting the ancestral origin of the sperm conjugation. This group represents the new order of primitive crustaceans, the Nectiopoda (Yager, 1981), discovered in marine caves of the Caribbean islands, and of Australia. The species *Speleonectes benjamini* has flagellated sperm with a 9 + 2 axoneme. They move towards the deferent ducts associated to form short spermatozeugmata consisting of 3–6 sperm cells.

In conclusion, this study advances our understanding of sperm structure in Carabidae and supports the notion that singleton (free) sperm are more common in basal Carabidae (see Gómez and Maddison, 2020) than in higher Carabidae (Brachininae and Harpalinae), which includes Sphodrini. Further research is needed to determine which species possess free sperm and which retain sperm conjugation with spermatostyles. The unique organization of sperm components in the newly examined species will also be valuable for future comparative analyses of their relationships, which we intend to pursue in subsequent studies.

CRediT authorship contribution statement

Andrea Di Giulio: Writing – review & editing, Writing – original draft, Resources. **Pietro Lupetti:** Writing – review & editing, Writing – original draft, Investigation. **Pietro Brandmayr:** Writing – review &

editing, Writing – original draft, Resources. **Romano Dallai:** Writing – review & editing, Writing – original draft, Investigation, Conceptualization. **Mariangela Gentile:** Writing – review & editing, Writing – original draft, Investigation. **David Mercati:** Writing – review & editing, Writing – original draft, Visualization, Investigation.

Declaration of Generative AI and AI-assisted technologies in the writing process

During the preparation of this work the authors used Nature Research Assistant in order to correct the manuscript. After using this tool/service, the authors reviewed and edited the content as needed and takes full responsibility for the content of the published article.

Data availability

No data was used for the research described in the article.

References

Afzelius, B.A., Dallai, R., 1987. Conjugated spermatozoa. In: Mohri, H. (Ed.), New horizons in sperm cell research. Japan Sci. Soc. press, Gordon and Breach Sci. Publ, pp. 349–355.

Bawa, S.R., Kanwar, K.C., 1975. Fine structure of *Callosobruchus maculatus* spermatozoon. J. Submicrosc. Cytol. 7, 71–79.

Breland, O.P., Simmons, E., 1970. Preliminary studies of the spermatozoa and the male reproductive system of some whirligig beetle (Coleoptera: Gyrinidae). Entomol. N. 81, 101–110. ⟨https://www.biodiversitylibrary.org/page/2740904⟩.

Carcupino, M., Stocchino, A.G., Corso, G., Manca, I., Casale, A., 2002. Morphology of the male reproductive apparatus and spermatodesms formation in *Percus strictus strictus* (Coleoptera, Carabidae). In: van der Horst, G., Franken, D., Bornman, R., Bornman, T., Dyer, S. (Eds.), In: Proceedings of 9th international symposium on spermatology. Monduzzi Editore, Bologna, pp. 31–34.

Dallai, R., Afzelius, B.A., 1985. Membrane specializations in the paired spermatozoa of dytiscid water beetle. Tissue Cell 17, 561–572. https://doi.org/10.1016/0040-8166(85)90032-1.

Dallai, R., Mercati, D., Giglio, A., Lupetti, P., 2019. Sperm ultrastructure in several species of Carabidae beetles (Insecta, Adephaga) and their organization in spermatozeugmata. Arthropod Struct. Dev. 51, 1–13. https://doi.org/10.1016/j.asd.2019.05.001.

Dallai, R., Mercati, D., Fanciulli, P.P., Petrioli, A., Lupetti, P., 2020. New findings on the sperm ultrastructure of Carabidae (Insecta, Coleoptera). Arthropod Struct. Dev. 54, 100912. https://doi.org/10.1016/j.asd.2019.100912.

Dallai, R., Mercati, D., Fanciulli, P.P., Lupetti, P., 2023. The structure of the female genital system of the diving beetle *Scarodytes halensis* (Fabricius, 1787) (Hydroporinae, Dytiscidae), and the organization of the spermatheca and the spermathecal gland complex. Insects 14 (3), 282. https://doi.org/10.3390/insects14030282.

Fisher, H., Hoekstra, H., 2010. Competition drives cooperation among closely related sperm of deer mice. Nature 463, 801–803. https://doi.org/10.1038/nature08736.

Giglio, A., Mercati, D., Lupetti, P., Brandmayr, P., Dallai, R., 2024. The sperm structure of *Clinidium canaliculatum* (Costa): A contribution to the systematic position of Rhysodidae (Coleoptera: Carabidae). Arthropod Struct. Dev. 78, 101330. https://doi.org/10.1016/j.asd.2023.101330.

Giribet, G., Edgecombe, G.D., 2012. Reevaluating the arthropod tree of life. Annu. Rev. Entomol. 57, 167–186. https://doi.org/10.1146/annurev-ento-120710-100659.

Gómez, R.A., Maddison, D.R., 2020. Novelty and emergent patterns in sperm: Morphological diversity and evolution of spermatozoa and sperm conjugation in ground beetles (Coleoptera: Carabidae). J. Morphol. (8), 862–892. https://doi.org/10.1002/jmor.21144.

Gómez, R.A., Mercati, D., Lupetti, P., Fanciulli, P.P., Dallai, R., 2023. Morphology of male and female reproductive systems in the ground beetle *Apotomus* and the peculiar sperm ultrastructure of *A. rufus* (P. Rossi, 1790) (Coleoptera, Carabidae). Arthropod Struct. Dev. 72, 101217. https://doi.org/10.1016/j.asd.2022.101217.

Gómez, R.A., Dallai, R., Sims-West, D.J., Mercati, D., Sinka, R., Ahmed-Braimah, Y., Pitnick, S., Dorus, S., 2024. Proteomic diversification of spermatostyles among six species of whirligig beetles. Mol. Reprod. Dev. 91 (5), e23745. https://doi.org/10.1002/mrd.23745.

Gustafson, G.T., Miller, K.B., 2017. Systematics and evolution of the whirligig beetle tribe Dineutini (Coleoptera: Gyrinidae: Gyrininae). Zool. J. Linn. Soc. 181 (1), 118–150. https://doi.org/10.1093/zoolinnean/zlw014.

Hayashi, F., 1998. Sperm-cooperation in the fish-fly, *Parachaulioides japonicus*. Funct. Ecol. 12, 347–350. https://doi.org/10.1046/j.1365-2435.1998.00205.x.

Hayashi, F., Kamimura, Y., 2002. Sperm-bundles of Cicadomorpha insects (Homoptera). Nat. Environ. Sci. Res. 15, 9–15. https://doi.org/10.32280/nesr.15.0_9.

Higginson, D.M., Pitnick, S., 2011. Evolution of intra-ejaculate sperm interactions: do sperm cooperate? Biol. Rev. Camb. Philos. Soc. 86, 249–270. https://doi.org/10.1111/j.1469-185x.2010.00147.x.

Higginson, D.M., Miller, K.B., Segraves, K.A., Pitnick, S., 2012. Convergence, recurrence and diversification of complex sperm traits in diving beetles (Dytiscidae). Evolution 66 (5), 1650–1661. https://doi.org/10.1111/j.1558-5646.2011.01532.x.

Hodgson, A.N., Ferenz, H.J., Schneider, S., 2013. Formation of sperm bundles in *Pterostichus nigrita* (Coleoptera: Carabidae). Invertebr. Reprod. Dev. 57, 120–131. https://doi.org/10.1080/07924259.2012.695295.

Immler, S., Moore, H.D., Breed, W.G., Birkhead, T.R., 2007. By hook or by crook? Morphometry, competition and cooperation in rodent sperm. PLoS One 2 (1), e170. https://doi.org/10.1371/journal.pone.0000170.

Lupetti, P., Mercati, D., Giglio, A., Brandmayr, P., Dallai, R., 2024. The cap and the spermatostyle protecting the sperm bundle have a similar origin - ultrastructural study of the spermatogenesis from the ground beetle *Carabus (Chaetocarabus) lefebvrei* Dejean, 1826 (Adephaga Carabidae). Insects 15 (11), 864. https://doi.org/10.3390/insects15110864.

Moore, T., Moore, H.D., 2002. Marsupial sperm pairing: a case of 'sticky' green beards? Trends Ecol. Evol. 17, 112–113. https://doi.org/10.1016/S0169-5347(01)02425-9.

Pitnick, S., Wolfner, M.F., Dorus, S., 2020. Post-ejaculatory modifications to sperm (PEMS). Biol. Rev. 95, 365–392. https://doi.org/10.1111/brv.12569.

Regier, J.C., Shultz, J.W., Zwick, A., Hussey, A., Ball, B., Wetzer, R., Martin, J.W., Cunningham, C.W., 2010. Arthropod relationships revealed by phylogenomic analysis of nuclear protein-coding sequences. Nature 463, 1079–1083. https://doi.org/10.1038/nature08742.

Sasakawa, K., 2007. Sperm bundle and reproductive organs of carabid beetles tribe Pterostichini (Coleoptera, Carabidae). Naturwissenschaften 94, 384–391. https://doi.org/10.1007/s00114-006-0200-4.

Sasakawa, K., 2009. Marked sperm dimorphism in the ground beetle *Scarites terricola*: a novel type of insect sperm polymorphism. Physiol. Entomol. 34, 387–390. https://doi.org/10.1111/j.1365-3032.2009.00694.x.

Schubert, L.F., Krüger, S., Moritz, G.B., Schubert, V., 2017. Male reproductive system and spermatogenesis of *Limodromus assimilis* (Paykull 1790). PloS One 12 (7), e0180492. https://doi.org/10.1371/journal.pone.0180492.

Takami, Y., 2002. Mating behavior, insemination and sperm transfer in the ground beetle *Carabus insulicola*. Zool. Sci. 19, 1067–1073. https://doi.org/10.2108/zsj.19.1067.

Takami, Y., Sota, T., 2007. Sperm competition promotes diversity of sperm bundles in Ohomopterus ground beetles. Naturwissenschaften 94, 543–550. https://doi.org/10.1007/s00114-007-0225-3.

Thiéry, J.P., 1967. Mise évidence des polysaccharides sur coupes fines en microscopie electronique. J. Microsc. 6, 987–1018.

Tihelka, E., Cai, C., Giacomelli, M., Lozano-Fernandez, J., Rota-Stabelli, O., Huang, D., Engel, M.S., Donoghue, P.C.J., Pisani, D., 2021. The evolution of insect biodiversity. Curr. Biol. 31, R1299–R1311. https://doi.org/10.1016/j.cub.2021.08.057.

von Reumont, B.M., Meusemann, K., Szucsich, N.U., Dell'Ampio, E., Gowri-Shankar, V., Bartel, D., Simon, S., Letsch, H.O., Stocsits, R.R., Luan, Y.X., Wägele, J.W., Pass, G., Hadrys, H., Misof, B., 2009. Can comprehensive background knowledge be incorporated into substitution models to improve phylogenetic analyses? A case study on major arthropod relationships. BMC Evol. Biol. 9, 119. https://doi.org/10.1186/1471-2148-9-119.

Werner, G., 1965. Untersuchungen über die spermiogenese beim sandläufer, *Cicindela campestris* L. Z. Zellforch. Mikrosk. Anat. Abt. Histochem 66, 255–275.

Woolley, D.M., Crockett, R.F., Groom, W.D., Revell, S.G., 2009. A study of synchronisation between the flagella of bull spermatozoa, with related observations. J. Exp. Biol. 212 (14), 2215–2223. https://doi.org/10.1242/jeb.028266.

Yager, J., 1981. A new class of Crustacea from a marine cave in the Bahamas. J. Crust. Biol. 1, 328–333. ⟨http://www.jstor.org/pss/1547965⟩.

Yager, J., 1989. The male reproductive system, sperm, and spermatophores of the primitive, hermaphroditic, remipede crustacean *Speleonectes benjamini*. Invertebr. Reprod. Dev. 15 (1), 75–81. https://doi.org/10.1080/07924259.1989.9672024.